DUNES TO YARDANGS: DEPOSITION AND EROSION IN SYRIA AND DAEDALIA PLANA, MARS.

K. D. Runyon[1], C. E. Viviano[1], and M. D. Day[2], [1]Johns Hopkins APL, Laurel, MD, USA (kirby.runyon@jhuapl.edu), [2]UCLA, Dept. Earth, Planetary, and Space Sciences.

Introduction: Geologically, Mars is an aeolian-dominated planet in its current and recent epochs. Constructional landforms (dunes and ripples) are common occurrences in craters and on some cratered plains [e.g., 1,2,3,4,5,6]. Sand-sculpted rocks and outcrops—yardangs and ventifacts—also feature prominently across Mars as seen at both orbital and rover scales [e.g., 7,8]. Vast amounts of lithified sediment across Mars – now sandstones and perhaps duststone, such as the Medusae Fossae Formation— [e.g., 9,10], have in many cases been eroded into yardangs.

This current work is partly motivated by a model [11] suggesting a light-toned, ridge-forming lithologic unit is the result of direct-deposition of wind-suspended dust immediately downwind of topographic obstacles. In Geissler's hypothesis, this results, broadly, in the formation of two bedform types: triangular-shaped "deltoids" in which the blunt end faces upwind with the tapered end pointing downwind; and sinuous ridges. These bedforms would be composed of cohesive dust and were interpreted to be the progenitors to Transverse Aeolian Ridges (TARs)—low mobility bedforms intermediate in size between meter-scale ripples and dunes [12]. In the present work, we build off this hypothesis, modifying and rejecting parts of it, informed from studies of dunes and yardangs elsewhere on Earth and Mars: we test the hypothesis that light-toned ridges previously interpreted as TAR progenitors are lithified paleo linear and possibly barchan dunes that have been eroded and may not be genetically related to TARs.

Geologic Context: The light-toned unit that is the focus of this study is within Syria and Daedalia plana and forms ridges and discrete delta-shaped landforms. The Arsia Mons volcano sits roughly 800 km to the west, and is constructed of both fluidized lava flows and pyroclastic ash deposits [13,14]. The light-toned unit crops out as discrete patches throughout the region. Western Syria Planum has been mapped as "Late Hesperian Volcanic Unit" of largely undifferentiated flows and source vents [15,16]. Patches of the light-toned unit were broadly mapped as "thin aeolian deposits" [17] but each patch was not mapped individually.

Methods: *Mapping:* In ArcMap 10, we mapped the occurrences of the light toned lithology in Syria and Daedalia Plana at a scale of 1:250,000 using the USGS THEMIS daytime IR Controlled Mosaic [100 m/pixel; 18]. High resolution images (25-50 cm/pixel) from the High Resolution Imaging Science Experiment (HiRISE)[19] allowed inspection of fine-scale morphology and stratigraphic relationships with the surrounding Hesperian-age lava flows at cm-to-m scales.

Composition: We used compositional data from the Compact Reconnaissance Imaging Spectrometer for Mars (CRISM) targeted hyperspectral mode. Mapping data were custom-processed and mosaicked using a processing pipeline in development during this study to produce the next-generation of mapping data tiles. Compared to previously released tiled multispectral mapping data, noise is strongly remediated and inter-strip residuals from atmospheric variations are minimized [20].

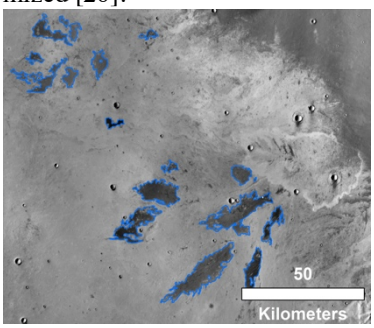

Fig. 1. Portion of mapped light-toned unit in Syria Planum.

Observations: *Geomorphology:* Broadly, the light-toned unit can be categorized into two groups: sinuous lineaments and isolated deltoids (Fig. 2; [11]). The sinuous lineaments are 10-100s m-long segments and commonly terminate in pairs with the tips curved toward each other. Wavelengths are 41 ± 11 m with heights of 2.6 ± 1.1 m. Crest lines commonly end in bifurcations or "Y-junctions;" deltoids are of the order 10 m long and are blunt toward the north and tapered toward the south, interpreted as the downwind direction.

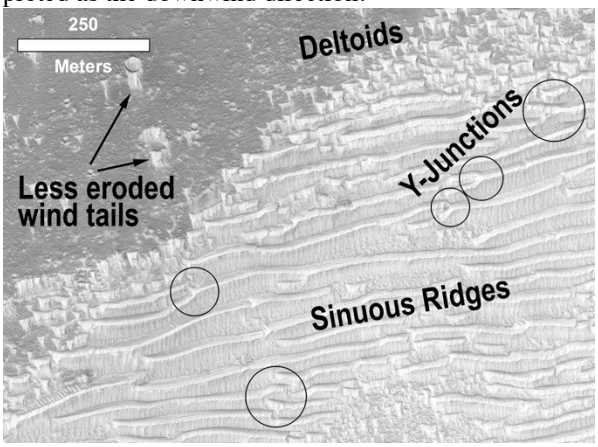

Fig. 2. The light-toned unit in Syria Planum (12.86°S, 254.16°E). The crestline terminations (e.g., Y-junctions) are reminiscent of transverse dunes with the deltoids resembling discrete dunes, such as barchans. The ridge spacing is in the mid-10s of meters, compared with mid-100s of meters for morphologically similar transverse dunes. Subset of HiRISE image ESP_056629_1670. Credit: NASA/JPL/UA.

The light-toned unit superposes crops out with sharp contacts against the flood lavas. The lavas appear to embay previous craters, muting their topography. Crater rims are commonly rimmed with the light-toned unit with down-wind pointing tails. Light-toned unit occurrences on crater floors are also common.

Composition: Spectra from a point location in an example overlapping targeted observation is plotted with an example dust spectrum for comparison (Fig. 3). We observe an association of dust-like spectra with the ridges, while surrounding material exhibit a mafic signature (pyroxene and olivine-bearing).

Fig. 3. CRISM targeted spectra from FRT0000986A of light-toned lithology as compared to an average CRISM dust spectrum from Tharsis [21].

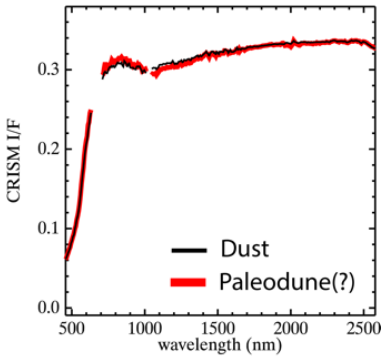

Discussion: The morphological similarities of the light-toned ridges to linear dunes are striking: both the ridges and linear dunes are sublinear with curved tips (defects) and Y-junctions (Fig. 2). Their dusty composition is consistent with a pyroclastic origin. We hypothesize pyroclastic ashfalls form the light-toned unit, which was then wind-mobilized into bedforms. Immobility promoted diagenetic alteration, perhaps aided by obliquity- and ice-driven ion mobilization [e.g., 9,22, 23]. Once lithified, the once-bedforms abraded as bedrock, and some of the features (barchan dunes?) eroded into nearly teardrop-shaped yardangs, forming the deltoids. Integrating our observations, we hypothesize the following sequence of events:

1. Lava embayed craters and muted topography.
2. Pyroclastic ash erupted onto the lava plains.
3. The high volume of volcaniclastic sediment was wind-mobilized and formed continuous transverse (and barchan?) dunes. Their tight spacing (~1/10th modern Martian transverse dunes) may be a function of finer grain sizes or their mode of emplacement, e.g., geologically instantaneously in a pyroclastic density current (e.g., [24]).
4. Following the final regional pyroclastic eruption, the sediment source stopped increasing, and the dunes equilibrated to consistent boundary conditions. [25,26].
5. Salts, particularly Cl and S, cemented [9,22,27] sand/dust grains into lithified sandstone/duststone. Such salts have been detected in the nearby Medusae Fossae Formation ignimbrite [10].
6. Low volumes of wind-blown sediment over time have continually eroded the volcaniclastic sandstone to the present as yardangs, exhuming the older lava flows.

Conclusion: We hypothesize the dust-like, bright-toned unit was emplaced pyroclastically and formed bedforms either in the pyroclastic deposition process or later by regional winds. We interpret modern abrasion by wind-mobilized sand has turned the lithified bedforms into yardangs. If this is true, an open question relates to the lack of observed sand.

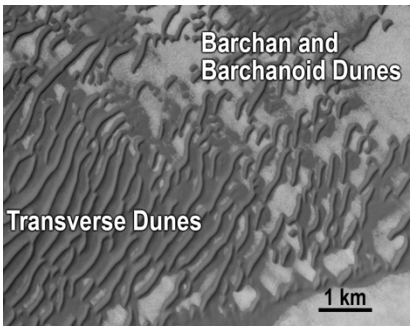

Fig. 4. Proposed modern dune field analog for the bright ridges and deltoids, though the dune spacing is ~one order of magnitude greater here. This view is in highland plains near 63.2°S, 159°E in Terra Cimmeria. CTX image G12_022994_1168_XN_63S201W. Credit: NASA/JPL/MSSS.

Acknowledgments: NASA funding from MDAP NNX16AJ43G/123117 for KDR and CEV.

References: **[1]** Sagan, C., et al., (1972). Icarus, 17(2), 346-372. **[2]** Edgett, K. S., & Lancaster, N. (1993). Journal of Arid Environments, 25(3), 271-297. **[3]** Bridges, N. T., et al., (2012). Nature, 485(7398), 339. **[4]** Runyon, K. D., et al., (2017). Aeolian research, 29, 1-11. **[5]** Runyon, K. D., et al., (2017). EPSL, 457, 204-212. **[6]** Banks, M. E., et al., (2018). JGR-P, 123(12), 3205-3219. **[7]** Bradley, B. A., et al., (2002). JGR-P, 107(E8), 2-1. **[8]** Mandt, K. E., et al., (2008). JGR-P, 113(E12). **[9]** Bridges, N. T., et al., (2010). Icarus, 205(1), 165-182. **[10]** Ojha, L., et al., (2018). Nature communications, 9(1), 2867.**[11]** Geissler, P. E. (2014). JGR-P, 119(12), 2583-2599.[12] Bourke, M.C., et al. (2003). LPSC Abstract #2090. **[13]** Mouginis-Mark, P. J. (2002). GRL, 29(16), 15-1. **[14]** Richardson, J. A., et al., (2017). EPSL, 458, 170-178. **[15]** Witbeck, N.E., et al., 1991 U.S. Geological Survey Atlas of Mars, 1:2,000,000 Geologic Series, M2M – 10/45 G, Map I-2010. **[16]** Tanaka, K.L., et al., 2014. U.S. Geological Survey Scientific Investigations Map 3292, scale 1:20,000,000, pamphlet 43 p. **[17]** Masursky, H., et al., (1978), Phoenicis Lacus Quadrangle, M 5M-15/112G, I-896 MC-17. **[18]** Fergason, R. L., et al. (2013, March). LPSC Abstract #1642. **[19]** McEwen, A. S., et al., (2007). JGR-P, 112(E5). **[20]** Seelos, F. P., et al., (2019, June). In 4th Planetary Data Workshop (Vol. 2151). **[21]** Viviano, C. E., et al. (2019). Icarus, 328, 274-286. **[22]** Clark, B. C. (1982). Analysis and interpretation of Viking inorganic chemistry data. **[23]** Jakosky, B. M., & Christensen, P. R. (1986). JGR-SR, 91(B3), 3547-3559. **[24]** Douillet, G. A., et al., (2013). Bulletin of volcanology, 75(11), 765. **[25]** Ewing, R. C., & Kocurek, G. (2010). Geomorphology, 114(3), 175-187. **[26]** Kocurek, G., Ewing, R. C., & Mohrig, D. (2010). ESPL, 35(1), 51-63. **[27]** Keller, J. M., et al., (2006). JGR-P, 111(E3).